Measurement of the branching fraction for the decay $\psi(3686) \to \phi K_S^0 K_S^0$

M. Ablikim,[1] M. N. Achasov,[13,b] P. Adlarson,[73] R. Aliberti,[34] A. Amoroso,[72a,72c] M. R. An,[38] Q. An,[69,56] Y. Bai,[55] O. Bakina,[35] I. Balossino,[29a] Y. Ban,[45,g] V. Batozskaya,[1,43] K. Begzsuren,[31] N. Berger,[34] M. Bertani,[28a] D. Bettoni,[29a] F. Bianchi,[72a,72c] E. Bianco,[72a,72c] J. Bloms,[66] A. Bortone,[72a,72c] I. Boyko,[35] R. A. Briere,[5] A. Brueggemann,[66] H. Cai,[74] X. Cai,[1,56] A. Calcaterra,[28a] G. F. Cao,[1,61] N. Cao,[1,61] S. A. Cetin,[60a] J. F. Chang,[1,56] T. T. Chang,[75] W. L. Chang,[1,61] G. R. Che,[42] G. Chelkov,[35,a] C. Chen,[42] Chao Chen,[53] G. Chen,[1] H. S. Chen,[1,61] M. L. Chen,[1,56,61] S. J. Chen,[41] S. M. Chen,[59] T. Chen,[1,61] X. R. Chen,[30,61] X. T. Chen,[1,61] Y. B. Chen,[1,56] Y. Q. Chen,[33] Z. J. Chen,[25,h] W. S. Cheng,[72c] S. K. Choi,[10] X. Chu,[42] G. Cibinetto,[29a] S. C. Coen,[4] F. Cossio,[72c] J. J. Cui,[48] H. L. Dai,[1,56] J. P. Dai,[77] A. Dbeyssi,[19] R. E. de Boer,[4] D. Dedovich,[35] Z. Y. Deng,[1] A. Denig,[34] I. Denysenko,[35] M. Destefanis,[72a,72c] F. De Mori,[72a,72c] B. Ding,[64,1] X. X. Ding,[45,g] Y. Ding,[39] Y. Ding,[33] J. Dong,[1,56] L. Y. Dong,[1,61] M. Y. Dong,[1,56,61] X. Dong,[74] S. X. Du,[79] Z. H. Duan,[41] P. Egorov,[35,a] Y. L. Fan,[74] J. Fang,[1,56] S. S. Fang,[1,61] W. X. Fang,[1] Y. Fang,[1] R. Farinelli,[29a] L. Fava,[72b,72c] F. Feldbauer,[4] G. Felici,[28a] C. Q. Feng,[69,56] J. H. Feng,[57] K Fischer,[67] M. Fritsch,[4] C. Fritzsch,[66] C. D. Fu,[1] Y. W. Fu,[1] H. Gao,[61] Y. N. Gao,[45,g] Yang Gao,[69,56] S. Garbolino,[72c] I. Garzia,[29a,29b] P. T. Ge,[74] Z. W. Ge,[41] C. Geng,[57] E. M. Gersabeck,[65] A Gilman,[67] K. Goetzen,[14] L. Gong,[39] W. X. Gong,[1,56] W. Gradl,[34] S. Gramigna,[29a,29b] M. Greco,[72a,72c] M. H. Gu,[1,56] Y. T. Gu,[16] C. Y Guan,[1,61] Z. L. Guan,[22] A. Q. Guo,[30,61] L. B. Guo,[40] R. P. Guo,[47] Y. P. Guo,[12,f] A. Guskov,[35,a] W. Y. Han,[38] X. Q. Hao,[20] F. A. Harris,[63] K. K. He,[53] K. L. He,[1,61] F. H. Heinsius,[4] C. H. Heinz,[34] Y. K. Heng,[1,56,61] C. Herold,[58] T. Holtmann,[4] P. C. Hong,[12,f] G. Y. Hou,[1,61] X. T. Hou,[1,61] Y. R. Hou,[61] Z. L. Hou,[1] H. M. Hu,[1,61] J. F. Hu,[54,i] T. Hu,[1,56,61] Y. Hu,[1] G. S. Huang,[69,56] K. X. Huang,[57] L. Q. Huang,[30,61] X. T. Huang,[48] Y. P. Huang,[1] T. Hussain,[71] N Hüsken,[27,34] W. Imoehl,[27] M. Irshad,[69,56] J. Jackson,[27] S. Jaeger,[4] S. Janchiv,[31] J. H. Jeong,[10] Q. Ji,[1] Q. P. Ji,[20] X. B. Ji,[1,61] X. L. Ji,[1,56] Y. Y. Ji,[48] Z. K. Jia,[69,56] P. C. Jiang,[45,g] S. S. Jiang,[38] T. J. Jiang,[17] X. S. Jiang,[1,56,61] Y. Jiang,[61] J. B. Jiao,[48] Z. Jiao,[23] S. Jin,[41] Y. Jin,[64] M. Q. Jing,[1,61] T. Johansson,[73] S. Kabana,[32] N. Kalantar-Nayestanaki,[62] X. L. Kang,[9] X. S. Kang,[39] R. Kappert,[62] M. Kavatsyuk,[62] B. C. Ke,[79] A. Khoukaz,[66] R. Kiuchi,[1] R. Kliemt,[14] L. Koch,[36] O. B. Kolcu,[60a] B. Kopf,[4] M. Kuessner,[4] X. Kui,[1] A. Kupsc,[43,73] W. Kühn,[36] J. J. Lane,[65] J. S. Lange,[36] P. Larin,[19] A. Lavania,[26] L. Lavezzi,[72a,72c] T. T. Lei,[69,k] Z. H. Lei,[69,56] H. Leithoff,[34] M. Lellmann,[34] T. Lenz,[34] C. Li,[46] C. Li,[42] C. H. Li,[38] Cheng Li,[69,56] D. M. Li,[79] F. Li,[1,56] G. Li,[1] H. Li,[69,56] H. B. Li,[1,61] H. J. Li,[20] H. N. Li,[54,i] Hui Li,[42] J. R. Li,[59] J. S. Li,[57] J. W. Li,[48] Ke Li,[1] L. J Li,[1,61] L. K. Li,[1] Lei Li,[3] M. H. Li,[42] P. R. Li,[37,j,k] S. X. Li,[12] T. Li,[48] W. D. Li,[1,61] W. G. Li,[1] X. H. Li,[69,56] X. L. Li,[48] Xiaoyu Li,[1,61] Y. G. Li,[45,g] Z. J. Li,[57] Z. X. Li,[16] Z. Y. Li,[57] C. Liang,[41] H. Liang,[69,56] H. Liang,[33] H. Liang,[1,61] Y. F. Liang,[52] Y. T. Liang,[30,61] G. R. Liao,[15] L. Z. Liao,[48] J. Libby,[26] A. Limphirat,[58] D. X. Lin,[30,61] T. Lin,[1] B. J. Liu,[1] B. X. Liu,[74] C. Liu,[33] C. X. Liu,[1] D. Liu,[19,69] F. H. Liu,[51] Fang Liu,[1] Feng Liu,[6] G. M. Liu,[54,i] H. Liu,[37,j,k] H. B. Liu,[16] H. M. Liu,[1,61] Huanhuan Liu,[1] Huihui Liu,[21] J. B. Liu,[69,56] J. L. Liu,[70] J. Y. Liu,[1,61] K. Liu,[1] K. Y. Liu,[39] Ke Liu,[22] L. Liu,[69,56] L. C. Liu,[42] Lu Liu,[42] M. H. Liu,[12,f] P. L. Liu,[1] Q. Liu,[61] S. B. Liu,[69,56] T. Liu,[12,f] W. K. Liu,[42] W. M. Liu,[69,56] X. Liu,[37,j,k] Y. Liu,[37,j,k] Y. B. Liu,[42] Z. A. Liu,[1,56,61] Z. Q. Liu,[48] X. C. Lou,[1,56,61] F. X. Lu,[57] H. J. Lu,[23] J. G. Lu,[1,56] X. L. Lu,[1] Y. Lu,[7] Y. P. Lu,[1,56] Z. H. Lu,[1,61] C. L. Luo,[40] M. X. Luo,[78] T. Luo,[12,f] X. L. Luo,[1,56] X. R. Lyu,[61] Y. F. Lyu,[42] F. C. Ma,[39] H. L. Ma,[1] J. L. Ma,[1,61] L. L. Ma,[48] M. M. Ma,[1,61] Q. M. Ma,[1] R. Q. Ma,[1,61] R. T. Ma,[61] X. Y. Ma,[1,56] Y. Ma,[45,g] F. E. Maas,[19] M. Maggiora,[72a,72c] S. Maldaner,[4] S. Malde,[67] A. Mangoni,[28b] Y. J. Mao,[45,g] Z. P. Mao,[1] S. Marcello,[72a,72c] Z. X. Meng,[64] J. G. Messchendorp,[14,62] G. Mezzadri,[29a] H. Miao,[1,61] T. J. Min,[41] R. E. Mitchell,[27] X. H. Mo,[1,56,61] N. Yu. Muchnoi,[13,b] Y. Nefedov,[35] F. Nerling,[19,d] I. B. Nikolaev,[13,b] Z. Ning,[1,56] S. Nisar,[11,l] Y. Niu,[48] S. L. Olsen,[61] Q. Ouyang,[1,56,61] S. Pacetti,[28b,28c] X. Pan,[53] Y. Pan,[55] A. Pathak,[33] Y. P. Pei,[69,56] M. Pelizaeus,[4] H. P. Peng,[69,56] K. Peters,[14,d] J. L. Ping,[40] R. G. Ping,[1,61] S. Plura,[34] S. Pogodin,[35] V. Prasad,[32] F. Z. Qi,[1] H. Qi,[69,56] H. R. Qi,[59] M. Qi,[41] T. Y. Qi,[12,f] S. Qian,[1,56] W. B. Qian,[61] C. F. Qiao,[61] J. J. Qin,[70] L. Q. Qin,[15] X. P. Qin,[12,f] X. S. Qin,[48] Z. H. Qin,[1,56] J. F. Qiu,[1] S. Q. Qu,[59] C. F. Redmer,[34] K. J. Ren,[38] A. Rivetti,[72c] V. Rodin,[62] M. Rolo,[72c] G. Rong,[1,61] Ch. Rosner,[19] S. N. Ruan,[42] N. Salone,[43] A. Sarantsev,[35,c] Y. Schelhaas,[34] K. Schoenning,[73] M. Scodeggio,[29a,29b] K. Y. Shan,[12,f] W. Shan,[24] X. Y. Shan,[69,56] J. F. Shangguan,[53] L. G. Shao,[1,61] M. Shao,[69,56] C. P. Shen,[12,f] H. F. Shen,[1,61] W. H. Shen,[61] X. Y. Shen,[1,61] B. A. Shi,[61] H. C. Shi,[69,56] J. Y. Shi,[1] Q. Q. Shi,[53] R. S. Shi,[1,61] X. Shi,[1,56] J. J. Song,[20] T. Z. Song,[57] W. M. Song,[33,1] Y. X. Song,[45,g] S. Sosio,[72a,72c] S. Spataro,[72a,72c] F. Stieler,[34] Y. J. Su,[61] G. B. Sun,[74] G. X. Sun,[1] H. Sun,[61] H. K. Sun,[1] J. F. Sun,[20] K. Sun,[59] L. Sun,[74] S. S. Sun,[1,61] T. Sun,[1,61] W. Y. Sun,[33] Y. Sun,[9] Y. J. Sun,[69,56] Y. Z. Sun,[1] Z. T. Sun,[48] Y. X. Tan,[69,56] C. J. Tang,[52] G. Y. Tang,[1] J. Tang,[57] Y. A. Tang,[74] L. Y Tao,[70] Q. T. Tao,[25,h] M. Tat,[67] J. X. Teng,[69,56] V. Thoren,[73] W. H. Tian,[57] W. H. Tian,[50] Y. Tian,[30,61] Z. F. Tian,[74] I. Uman,[60b] B. Wang,[1] B. L. Wang,[61] Bo Wang,[69,56] C. W. Wang,[41] D. Y. Wang,[45,g] F. Wang,[70] H. J. Wang,[37,j,k] H. P. Wang,[1,61] K. Wang,[1,56] L. L. Wang,[1] M. Wang,[48] Meng Wang,[1,61] S. Wang,[12,f] T. Wang,[12,f] T. J. Wang,[42] W. Wang,[57] W. Wang,[70] W. H. Wang,[74] W. P. Wang,[69,56] X. Wang,[45,g] X. F. Wang,[37,j,k] X. J. Wang,[38] X. L. Wang,[12,f] Y. Wang,[59] Y. D. Wang,[44] Y. F. Wang,[1,56,61] Y. H. Wang,[46] Y. N. Wang,[44] Y. Q. Wang,[1] Yaqian Wang,[18,1] Yi Wang,[59] Z. Wang,[1,56] Z. L. Wang,[70] Z. Y. Wang,[1,61] Ziyi Wang,[61] D. Wei,[68] D. H. Wei,[15] F. Weidner,[66] S. P. Wen,[1] C. W. Wenzel,[4] U. Wiedner,[4]

G. Wilkinson,[67] M. Wolke,[73] L. Wollenberg,[4] C. Wu,[38] J. F. Wu,[1,61] L. H. Wu,[1] L. J. Wu,[1,61] X. Wu,[12,f] X. H. Wu,[33] Y. Wu,[69] Y. J Wu,[30] Z. Wu,[1,56] L. Xia,[69,56] X. M. Xian,[38] T. Xiang,[45,g] D. Xiao,[37,j,k] G. Y. Xiao,[41] H. Xiao,[12,f] S. Y. Xiao,[1] Y. L. Xiao,[12,f] Z. J. Xiao,[40] C. Xie,[41] X. H. Xie,[45,g] Y. Xie,[48] Y. G. Xie,[1,56] Y. H. Xie,[6] Z. P. Xie,[69,56] T. Y. Xing,[1,61] C. F. Xu,[1,61] C. J. Xu,[57] G. F. Xu,[1] H. Y. Xu,[64] Q. J. Xu,[17] W. L. Xu,[64] X. P. Xu,[53] Y. C. Xu,[76] Z. P. Xu,[41] F. Yan,[12,f] L. Yan,[12,f] W. B. Yan,[69,56] W. C. Yan,[79] X. Q Yan,[1] H. J. Yang,[49,e] H. L. Yang,[33] H. X. Yang,[1] Tao Yang,[1] Y. Yang,[12,f] Y. F. Yang,[42] Y. X. Yang,[1,61] Yifan Yang,[1,61] M. Ye,[1,56] M. H. Ye,[8] J. H. Yin,[1] Z. Y. You,[57] B. X. Yu,[1,56,61] C. X. Yu,[42] G. Yu,[1,61] T. Yu,[70] X. D. Yu,[45,g] C. Z. Yuan,[1,61] L. Yuan,[2] S. C. Yuan,[1] X. Q. Yuan,[1] Y. Yuan,[1,61] Z. Y. Yuan,[57] C. X. Yue,[38] A. A. Zafar,[71] F. R. Zeng,[48] X. Zeng,[12,f] Y. Zeng,[25,h] Y. J. Zeng,[1,61] X. Y. Zhai,[33] Y. H. Zhan,[57] A. Q. Zhang,[1,61] B. L. Zhang,[1,61] B. X. Zhang,[1] D. H. Zhang,[42] G. Y. Zhang,[20] H. Zhang,[69] H. H. Zhang,[33] H. H. Zhang,[57] H. Q. Zhang,[1,56,61] H. Y. Zhang,[1,56] J. J. Zhang,[50] J. L. Zhang,[75] J. Q. Zhang,[40] J. W. Zhang,[1,56,61] J. X. Zhang,[37,j,k] J. Y. Zhang,[1] J. Z. Zhang,[1,61] Jiawei Zhang,[1,61] L. M. Zhang,[59] L. Q. Zhang,[57] Lei Zhang,[41] P. Zhang,[1] Q. Y. Zhang,[38,79] Shuihan Zhang,[1,61] Shulei Zhang,[25,h] X. D. Zhang,[44] X. M. Zhang,[1] X. Y. Zhang,[53] X. Y. Zhang,[48] Y. Zhang,[67] Y. T. Zhang,[79] Y. H. Zhang,[1,56] Yan Zhang,[69,56] Yao Zhang,[1] Z. H. Zhang,[1] Z. L. Zhang,[33] Z. Y. Zhang,[74] Z. Y. Zhang,[42] G. Zhao,[1] J. Zhao,[38] J. Y. Zhao,[1,61] J. Z. Zhao,[1,56] Lei Zhao,[69,56] Ling Zhao,[1] M. G. Zhao,[42] S. J. Zhao,[79] Y. B. Zhao,[1,56] Y. X. Zhao,[30,61] Z. G. Zhao,[69,56] A. Zhemchugov,[35,a] B. Zheng,[70] J. P. Zheng,[1,56] W. J. Zheng,[1,61] Y. H. Zheng,[61] B. Zhong,[40] X. Zhong,[57] H. Zhou,[48] L. P. Zhou,[1,61] X. Zhou,[74] X. K. Zhou,[6] X. R. Zhou,[69,56] X. Y. Zhou,[38] Y. Z. Zhou,[12,f] J. Zhu,[42] K. Zhu,[1] K. J. Zhu,[1,56,61] L. Zhu,[33] L. X. Zhu,[61] S. H. Zhu,[68] S. Q. Zhu,[41] T. J. Zhu,[12,f] W. J. Zhu,[12,f] Y. C. Zhu,[69,56] Z. A. Zhu,[1,61] J. H. Zou,[1] and J. Zu[69,56]

(BESIII Collaboration)

[1]*Institute of High Energy Physics, Beijing 100049, People's Republic of China*
[2]*Beihang University, Beijing 100191, People's Republic of China*
[3]*Beijing Institute of Petrochemical Technology, Beijing 102617, People's Republic of China*
[4]*Bochum Ruhr-University, D-44780 Bochum, Germany*
[5]*Carnegie Mellon University, Pittsburgh, Pennsylvania 15213, USA*
[6]*Central China Normal University, Wuhan 430079, People's Republic of China*
[7]*Central South University, Changsha 410083, People's Republic of China*
[8]*China Center of Advanced Science and Technology, Beijing 100190, People's Republic of China*
[9]*China University of Geosciences, Wuhan 430074, People's Republic of China*
[10]*Chung-Ang University, Seoul, 06974, Republic of Korea*
[11]*COMSATS University Islamabad, Lahore Campus, Defence Road, Off Raiwind Road, 54000 Lahore, Pakistan*
[12]*Fudan University, Shanghai 200433, People's Republic of China*
[13]*G.I. Budker Institute of Nuclear Physics SB RAS (BINP), Novosibirsk 630090, Russia*
[14]*GSI Helmholtzcentre for Heavy Ion Research GmbH, D-64291 Darmstadt, Germany*
[15]*Guangxi Normal University, Guilin 541004, People's Republic of China*
[16]*Guangxi University, Nanning 530004, People's Republic of China*
[17]*Hangzhou Normal University, Hangzhou 310036, People's Republic of China*
[18]*Hebei University, Baoding 071002, People's Republic of China*
[19]*Helmholtz Institute Mainz, Staudinger Weg 18, D-55099 Mainz, Germany*
[20]*Henan Normal University, Xinxiang 453007, People's Republic of China*
[21]*Henan University of Science and Technology, Luoyang 471003, People's Republic of China*
[22]*Henan University of Technology, Zhengzhou 450001, People's Republic of China*
[23]*Huangshan College, Huangshan 245000, People's Republic of China*
[24]*Hunan Normal University, Changsha 410081, People's Republic of China*
[25]*Hunan University, Changsha 410082, People's Republic of China*
[26]*Indian Institute of Technology Madras, Chennai 600036, India*
[27]*Indiana University, Bloomington, Indiana 47405, USA*
[28a]*INFN Laboratori Nazionali di Frascati, I-00044, Frascati, Italy*
[28b]*INFN Sezione di Perugia, I-06100, Perugia, Italy*
[28c]*University of Perugia, I-06100, Perugia, Italy*
[29a]*INFN Sezione di Ferrara, I-44122, Ferrara, Italy*
[29b]*University of Ferrara, I-44122, Ferrara, Italy*
[30]*Institute of Modern Physics, Lanzhou 730000, People's Republic of China*
[31]*Institute of Physics and Technology, Peace Avenue 54B, Ulaanbaatar 13330, Mongolia*
[32]*Instituto de Alta Investigación, Universidad de Tarapacá, Casilla 7D, Arica, Chile*
[33]*Jilin University, Changchun 130012, People's Republic of China*
[34]*Johannes Gutenberg University of Mainz, Johann-Joachim-Becher-Weg 45, D-55099 Mainz, Germany*

[35]Joint Institute for Nuclear Research, 141980 Dubna, Moscow region, Russia
[36]Justus-Liebig-Universitaet Giessen, II. Physikalisches Institut, Heinrich-Buff-Ring 16, D-35392 Giessen, Germany
[37]Lanzhou University, Lanzhou 730000, People's Republic of China
[38]Liaoning Normal University, Dalian 116029, People's Republic of China
[39]Liaoning University, Shenyang 110036, People's Republic of China
[40]Nanjing Normal University, Nanjing 210023, People's Republic of China
[41]Nanjing University, Nanjing 210093, People's Republic of China
[42]Nankai University, Tianjin 300071, People's Republic of China
[43]National Centre for Nuclear Research, Warsaw 02-093, Poland
[44]North China Electric Power University, Beijing 102206, People's Republic of China
[45]Peking University, Beijing 100871, People's Republic of China
[46]Qufu Normal University, Qufu 273165, People's Republic of China
[47]Shandong Normal University, Jinan 250014, People's Republic of China
[48]Shandong University, Jinan 250100, People's Republic of China
[49]Shanghai Jiao Tong University, Shanghai 200240, People's Republic of China
[50]Shanxi Normal University, Linfen 041004, People's Republic of China
[51]Shanxi University, Taiyuan 030006, People's Republic of China
[52]Sichuan University, Chengdu 610064, People's Republic of China
[53]Soochow University, Suzhou 215006, People's Republic of China
[54]South China Normal University, Guangzhou 510006, People's Republic of China
[55]Southeast University, Nanjing 211100, People's Republic of China
[56]State Key Laboratory of Particle Detection and Electronics, Beijing 100049, Hefei 230026, People's Republic of China
[57]Sun Yat-Sen University, Guangzhou 510275, People's Republic of China
[58]Suranaree University of Technology, University Avenue 111, Nakhon Ratchasima 30000, Thailand
[59]Tsinghua University, Beijing 100084, People's Republic of China
[60a]Turkish Accelerator Center Particle Factory Group, Istinye University, 34010, Istanbul, Turkey
[60b]Near East University, Nicosia, North Cyprus, 99138, Mersin 10, Turkey
[61]University of Chinese Academy of Sciences, Beijing 100049, People's Republic of China
[62]University of Groningen, NL-9747 AA Groningen, The Netherlands
[63]University of Hawaii, Honolulu, Hawaii 96822, USA
[64]University of Jinan, Jinan 250022, People's Republic of China
[65]University of Manchester, Oxford Road, Manchester M13 9PL, United Kingdom
[66]University of Muenster, Wilhelm-Klemm-Strasse 9, 48149 Muenster, Germany
[67]University of Oxford, Keble Road, Oxford OX13RH, United Kingdom
[68]University of Science and Technology Liaoning, Anshan 114051, People's Republic of China
[69]University of Science and Technology of China, Hefei 230026, People's Republic of China
[70]University of South China, Hengyang 421001, People's Republic of China
[71]University of the Punjab, Lahore-54590, Pakistan
[72a]University of Turin and INFN, University of Turin, I-10125, Turin, Italy
[72b]University of Eastern Piedmont, I-15121, Alessandria, Italy
[72c]INFN, I-10125, Turin, Italy
[73]Uppsala University, Box 516, SE-75120 Uppsala, Sweden
[74]Wuhan University, Wuhan 430072, People's Republic of China
[75]Xinyang Normal University, Xinyang 464000, People's Republic of China
[76]Yantai University, Yantai 264005, People's Republic of China
[77]Yunnan University, Kunming 650500, People's Republic of China
[78]Zhejiang University, Hangzhou 310027, People's Republic of China
[79]Zhengzhou University, Zhengzhou 450001, People's Republic of China

[a]Also at the Moscow Institute of Physics and Technology, Moscow 141700, Russia.
[b]Also at the Novosibirsk State University, Novosibirsk, 630090, Russia.
[c]Also at the NRC "Kurchatov Institute", PNPI, 188300, Gatchina, Russia.
[d]Also at Goethe University Frankfurt, 60323 Frankfurt am Main, Germany.
[e]Also at Key Laboratory for Particle Physics, Astrophysics and Cosmology, Ministry of Education; Shanghai Key Laboratory for Particle Physics and Cosmology; Institute of Nuclear and Particle Physics, Shanghai 200240, People's Republic of China.
[f]Also at Key Laboratory of Nuclear Physics and Ion-beam Application (MOE) and Institute of Modern Physics, Fudan University, Shanghai 200443, People's Republic of China.
[g]Also at State Key Laboratory of Nuclear Physics and Technology, Peking University, Beijing 100871, People's Republic of China.
[h]Also at School of Physics and Electronics, Hunan University, Changsha 410082, China.

(Received 16 March 2023; accepted 15 August 2023; published 5 September 2023)

Based on $(448.1 \pm 2.9) \times 10^6$ $\psi(3686)$ events collected with the BESIII detector operating at the BEPCII collider, the decay $\psi(3686) \to \phi K_S^0 K_S^0$ is observed for the first time. Taking the interference between $\psi(3686)$ decay and continuum production into account, the branching fraction of this decay is measured to be $\mathcal{B}(\psi(3686) \to \phi K_S^0 K_S^0) = (3.53 \pm 0.20 \pm 0.21) \times 10^{-5}$, where the first uncertainty is statistical and the second is systematic. Combining with the world average value for $\mathcal{B}(J/\psi \to \phi K_S^0 K_S^0)$, the ratio $\mathcal{B}(\psi(3686) \to \phi K_S^0 K_S^0)/\mathcal{B}(J/\psi \to \phi K_S^0 K_S^0)$ is determined to be $(6.0 \pm 1.6)\%$, which is suppressed relative to the 12% rule.

DOI: 10.1103/PhysRevD.108.052001

I. INTRODUCTION

The J/ψ and $\psi(3686)$ are nonrelativistic bound states of a charm and an anticharm quark, called charmonium. Experimental measurements of the decays of charmonium states ψ [which denotes both the J/ψ and $\psi(3686)$] can provide an ideal laboratory to study the dynamics of strong force physics, validate models and test various aspects of quantum chromodynamics (QCD) [1,2]. Since the discovery of the $\psi(3686)$ in 1974 [3], it has been studied for over 40 years. However, there are still problems and puzzles that need to be understood [4].

Perturbative QCD predicts that both the J/ψ and $\psi(3686)$ decay into light-hadron final states with a width proportional to the square of the wave function at the origin [5,6]. This yields the widely known "12% rule": $\mathcal{Q}_h = \mathcal{B}_{\psi(3686)\to h}/\mathcal{B}_{J/\psi\to h} \simeq \mathcal{B}_{\psi(3686)\to e^+e^-}/\mathcal{B}_{J/\psi\to e^+e^-} \simeq 13.3\%$ [7], where h denotes any exclusive hadronic decay mode. Although this relation is expected to hold to a reasonably good degree for both inclusive and exclusive decays [8], it fails severely in the case of vector-pseudoscalar meson final states, such as $\rho\pi$ [9]. With the recent experimental results on J/ψ and $\psi(3686)$ two-body decays, such as the vector-tensor channel [10], the pseudoscalar-pseudoscalar channel [11], baryon-antibaryon mode [12], and multibody decays such as $\phi\pi^+\pi^-$, $p\bar{p}\pi^0$ [13], etc., extensive tests of the 12% rule have been performed. The ratios $\mathcal{Q}_h$ for some decay modes are suppressed, some are enhanced, while others obey the 12% rule. More experimental results are still desirable to test the 12% rule and further investigate charmonium decay mechanisms [4].

In this work, we present the first observation and branching fraction (BF) measurement of the decay $\psi(3686) \to \phi K_S^0 K_S^0$ by analyzing $(448.1 \pm 2.9) \times 10^6$ $\psi(3686)$ events collected with the BESIII detector in 2009 and 2012 [14]. In addition, the 12% rule in the decay $\psi(3686) \to \phi K_S^0 K_S^0$ are tested.

II. BESIII EXPERIMENT AND MONTE CARLO SIMULATION

The BESIII detector [15] records symmetric e^+e^- collisions provided by the BEPCII [16] storage ring in the c.m. energy range from 2.00 GeV to 4.95 GeV, with a peak luminosity of 1×10^{33} cm^{-2} s^{-1} achieved at $\sqrt{s} = 3.77$ GeV.

The cylindrical core of the BESIII detector covers 93% of the full solid angle and consists of a helium-based multilayer drift chamber (MDC), a plastic scintillator time-of-flight (TOF) system, and a CsI(Tl) electromagnetic calorimeter (EMC), which are all enclosed in a superconducting solenoidal magnet providing a 1.0 T magnetic field. The solenoid is supported by an octagonal flux-return yoke with resistive plate counter muon identification modules interleaved with steel. The charged-particle momentum resolution at 1 GeV/c is 0.5%, and the dE/dx resolution is 6% for electrons from Bhabha scattering. The EMC measures photon energies with a resolution of 2.5% (5%) at 1 GeV in the barrel (end cap) region. The time resolution in the TOF barrel region is 68 ps, while that in the end cap region is 110 ps.

Simulated data samples produced with a Geant4-based [17] Monte Carlo (MC) package, which includes the geometric description of the BESIII detector [18,19] and the detector response, are used to determine detection efficiencies and to estimate backgrounds. The simulation models the beam energy spread and initial state radiation in the e^+e^- annihilations with the generator KKMC [20].

[i]Also at Guangdong Provincial Key Laboratory of Nuclear Science, Institute of Quantum Matter, South China Normal University, Guangzhou 510006, China.
[j]Also at Frontiers Science Center for Rare Isotopes, Lanzhou University, Lanzhou 730000, People's Republic of China.
[k]Also at Lanzhou Center for Theoretical Physics, Lanzhou University, Lanzhou 730000, People's Republic of China.
[l]Also at the Department of Mathematical Sciences, IBA, Karachi, Pakistan.

The inclusive MC sample includes the production of the $\psi(3686)$ resonance, the initial state radiation production of the J/ψ, and the continuum processes incorporated in KKMC [20]. All particle decays are modeled with EvtGen [21,22] using BFs either taken from the Particle Data Group (PDG) [7], when available, or otherwise estimated with LUNDCHARM [23,24]. Final state radiation from charged final state particles is incorporated using the PHOTOS package [25]. To determine the detection efficiency for the signal process, 2×10^5 signal MC samples are generated with a modified data-driven generator BODY3 [21,26], which could simulate contributions from different intermediate states in data for a given three-body final state. Data sets collected at center-of-mass energies ranging from 3.508 GeV to 3.773 GeV are used to estimate the contribution from continuum processes. The $\psi(3686)$ scan data sets ranging from 3.670 GeV to 3.710 GeV are used to estimate the phase angles between continuum processes and the $\psi(3686)$. The total integrated luminosity for all data except 3.773 GeV and psi(3686) scan data is 504.6 pb^{-1}, while the integrated luminosity for 3.773 GeV is 2931.8 pb^{-1} [27] and the average integrated luminosity for $\psi(3686)$ scan data is 92.2 pb^{-1}.

III. EVENT SELECTION AND DATA ANALYSIS

To select candidate events for $\psi(3686) \to \phi K_S^0 K_S^0$, the ϕ and K_S^0 mesons are reconstructed using their decays to K^+K^- and $\pi^+\pi^-$, respectively.

Each candidate signal event is required to have at least six charged tracks. The charged tracks detected in the MDC are required to be within a polar angle (θ) range of $|\cos\theta| < 0.93$, where θ is defined with respect to the z axis, which is the symmetry axis of the MDC. The charged tracks from the $\phi \to K^+K^-$ decay are required to have a distance of closest approach to the interaction point (IP) less than 10 cm along the z axis ($|V_z|$) and less than 1 cm in the transverse plane ($|V_{xy}|$). The $\mathrm{d}E/\mathrm{d}x$ information recorded by the MDC and the time-of-flight information in the TOF are used for particle identification (PID), and the charged tracks are assigned as kaons when the kaon hypothesis has a greater likelihood, *i.e.*, $\mathcal{L}(K) > \mathcal{L}(\pi)$.

The charged pions used for K_S^0 reconstruction are required to have a greater likelihood for the pion hypothesis, *i.e.*, $\mathcal{L}(\pi) > \mathcal{L}(K)$. Both pions must satisfy $|\cos\theta| < 0.93$ and $|V_z| < 20$ cm and their trajectories are constrained to originate from a common vertex by applying a vertex fit [28]. The invariant mass of the $\pi^+\pi^-$ pair $M_{\pi^+\pi^-}$ needs to be in the range $(0.45, 0.55)$ GeV/c^2. Here, $M_{\pi^+\pi^-}$ is calculated with the pions constrained to originate at the decay vertex. The K_S^0 candidate is then formed and the opposite direction of its momentum is constrained to point to the IP. The decay length of the K_S^0 candidate is required to be greater than twice the vertex resolution.

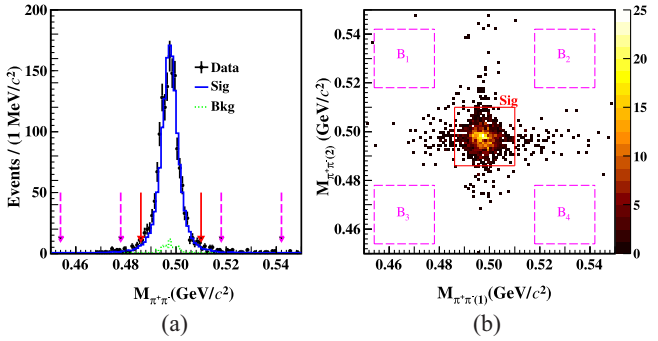

FIG. 1. (a) The distribution of $M_{\pi^+\pi^-}$, where the signal region is defined as $M_{\pi^+\pi^-} \in (0.486, 0.510)$ GeV/c^2 and the sideband regions are defined as $M_{\pi^+\pi^-} \in (0.454, 0.478)$ or $(0.518, 0.542)$ GeV/c^2, respectively. The black points with error bars are data. The blue solid curve is the signal MC. The green dashed curve is the inclusive MC. The pair of red arrows shows the signal region, and the two pairs of pink dashed arrows show the sideband region. (b) The 2D distribution of $M_{\pi^+\pi^-(1)}$ vs. $M_{\pi^+\pi^-(2)}$ (the subscripts 1 and 2 indicate the two $\pi^+\pi^-$ combinations, respectively) in the signal and sideband regions. The red solid rectangle shows the 2D signal region where both K_S^0 candidates are required to be in the range $(0.486, 0.510)$ GeV/c^2, and the pink dashed rectangles show the 2D sideband regions where both K_S^0 candidates are required to be in the range of $(0.454, 0.478)$ or $(0.518, 0.542)$ GeV/c^2.

A four-constraint (4C) kinematic fit imposing energy and momentum conservation is performed. The helix parameters of the charged tracks in the MC events are corrected to improve the consistency with data. The correction factors for $K^\pm$ are cited from Ref. [29], while the correction factors for $\pi^\pm$ are determined by studying the $\psi(3686) \to \pi^+\pi^- K_S^0 K_S^0$, $K_S^0 \to \pi^+\pi^-$ process. The events satisfying $\chi^2_{\mathrm{4C}} < 50$ are kept for further analysis. If there are multiple candidates in an event, the one with the smallest χ^2_{4C} is kept for further analysis.

Analysis of the $\psi(3686)$ inclusive MC sample with an event type examination tool, TopoAna [30], indicates that the main background events come from $\psi(3686) \to \pi^+\pi^- J/\psi$ with $J/\psi \to \phi\pi^+\pi^-$, $\phi \to K^+K^-$. The background events, however, do not contain a $K_S^0 K_S^0$ pair and can thus be described by $K_S^0 K_S^0$ sideband events. The one-dimensional distribution of $M_{\pi^+\pi^-}$ for the K_S^0 candidates in the signal and sideband regions is shown in Fig. 1(a). The two-dimensional (2D) $M_{\pi^+\pi^-}$ distribution for the two K_S^0 candidates is shown in Fig. 1(b), where the signal region in the red solid rectangle indicates that both K_S^0 candidates are required to satisfy $M_{\pi^+\pi^-} \in (0.486, 0.510)$ GeV/c^2 (marked as Sig). The size of the signal region corresponds to three times the resolution around the known K_S^0 mass [7]. The 2D sideband region is defined as $M_{\pi^+\pi^-} \in (0.454, 0.478)$ GeV/c^2 or $(0.518, 0.542)$ GeV/c^2 (marked as B_i with $i = 1, 2, 3, 4$), where both K_S^0 candidates lie in the sideband region.

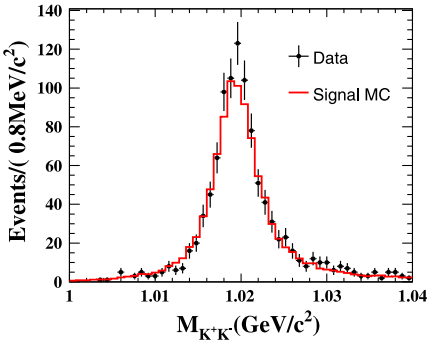

FIG. 2. The $M_{K^+K^-}$ distribution for the accepted candidates in the 2D K_S^0 signal region for the $\psi(3686)$ data. The black points with error bars are data. The red solid curve is the signal MC.

Figure 2 shows the distributions of $M_{K^+K^-}$ in the 2D K_S^0 signal region. The background rate determined by fitting to the $M_{K^+K^-}$ distributions was found to be extremely low, reaching a value of 10^{-6}. In the fit, the ϕ signal shape was described with the MC signal shape convolved with a parameter-floating Gaussian function, and the background was described with a first-order polynomial function. This low background level allows us to directly count the number of signal events in the 2D K_S^0 signal region without considering any significant background contributions. The number of net $\psi(3686) \to \phi K_S^0 K_S^0$ candidate events is given by $N_{\rm net}^{\psi(3686)} = N_{\rm sig}^{\psi(3686)}$-$N_{\rm bkg}^{\psi(3686)}$, where $N_{\rm sig}^{\psi(3686)}$ is determined by counting the events left in the 2D K_S^0 signal region and $N_{\rm bkg}^{\psi(3686)}$ is estimated with the mean value of the background events in the sideband regions defined in Fig. 1(b), *i.e.*, $N_{\rm bkg}^{\psi(3686)} = \sum B_i/4$ (with $i = 1, 2, 3, 4$). For $N_{\rm sig}^{\psi(3686)}$ and $N_{\rm bkg}^{\psi(3686)}$, the values are 1023 ± 32 and 0, respectively.

To investigate the background from the continuum processes [14] $e^+e^- \to \phi K_S^0 K_S^0$, the same selection criteria and sideband definition are applied on the off-resonance data samples. The obtained values of signal yields $N_{\rm net}$ from the continuum data samples are listed in Table I. A scale factor f_c is considered to account for the energy dependence of the cross section.

TABLE I. The continuum background estimation for each data set, where $E_{\rm CM}$ is the center-of-mass energy; $\mathcal{L}_{\rm cont}$ is the integrated luminosity, $N_{\rm net}$ is the number of signal events in the 2D K_S^0 signal region after subtracting the backgrounds estimated with the sideband method, f_c is the scale factor for each energy point, and $N_{\rm cont}$ is the continuum contribution calculated with $N_{\rm net} \times f_c$.

$E_{\rm CM}$ (GeV)	$\mathcal{L}_{\rm cont}$ (pb^{-1})	$N_{\rm net}$	f_c	$N_{\rm cont}$
3.508	183.64	32 ± 6	3.30	106 ± 20
3.510	181.79	28 ± 7	3.34	94 ± 23
3.539	25.50	7 ± 3	24.17	169 ± 72
3.553	42.56	10 ± 3	14.59	146 ± 44
3.554	27.24	1 ± 1	22.81	23 ± 23
3.650	43.88	14 ± 4	14.94	209 ± 60
3.773	2931.80	465 ± 22	0.24	112 ± 5

$$f_c = \frac{\mathcal{L}_{\psi(3686)}}{\mathcal{L}_{\rm cont}} \times \frac{s_{\rm cont}^n}{s_{\psi(3686)}^n}, \quad (1)$$

where $\mathcal{L}_{\psi(3686)}$ [14] and $\mathcal{L}_{\rm cont}$ are the integrated luminosities for the $\psi(3686)$ and continuum data samples, and $s_{\psi(3686)}$ and $s_{\rm cont}$ are the squares of the corresponding c.m. energies. We use $n = 1$ in the nominal result, which corresponds to a $1/s$ dependence for the continuum cross section. The impact of this assumption for n will be considered as a source of systematic uncertainty. The calculated results for $N_{\rm cont}$ estimated from different data sets are listed in the last column of Table I. To combine these different $N_{\rm cont}$ into an average combined result $\bar{N}_{\rm cont}$, we use a weighted average method where the weights for each $N_{\rm cont}$ are proportional to the inverse square of the corresponding uncertainties. The $\bar{N}_{\rm cont}$ is determined to be 108 ± 5.

Figure 3 shows the Dalitz plots for the accepted candidates in data and BODY3 signal MC samples. The one-dimensional projections of the Dalitz plots are shown in Fig. 4. The detection efficiency for $\psi(3686) \to \phi K_S^0 K_S^0$ is determined to be $(18.50 \pm 0.09)\%$, where the uncertainty comes from the MC statistics.

The interference between the $\psi(3686)$ decay and the continuum production $e^+e^- \to \phi K_S^0 K_S^0$ is considered by fitting to the cross sections in the vicinity of the $\psi(3686)$, followed the method in Ref [31]. The fit yields two solutions for the phase angle between the $\psi(3686)$ and continuum processes, corresponding to a constructive interference of $(83 \pm 11)^\circ$ and a destructive interference of $-(85 \pm 9)^\circ$ (with more details in Appendix). The former is determined to be the physical one by the isospin symmetry with the decay of $\psi(3686) \to \phi K^+ K^-$ [7]. The interference contribution is estimated by scaling the continuum contribution with the ratio of the cross sections between the interference term and the continuum process. It is determined to be $N_{\rm inter} = 228 \pm 24$.

The BF of $\psi(3686) \to \phi K_S^0 K_S^0$ is determined by

$$\mathcal{B}_{\psi(3686)\to\phi K_S^0 K_S^0} = \frac{N_{\rm net}^{\psi(3686)} - \bar{N}_{\rm cont} - N_{\rm inter}}{N_{\psi(3686)} \cdot \varepsilon \cdot \mathcal{B}_{\phi\to K^+K^-} \cdot \mathcal{B}^2_{K_S^0\to\pi^+\pi^-}}, \quad (2)$$

where $N_{\rm net}^{\psi(3686)} - \bar{N}_{\rm cont} - N_{\rm inter} = 687 \pm 40$ is the net number of $\psi(3686) \to \phi K_S^0 K_S^0$, $N_{\psi(3686)} = (448.1 \pm 2.9) \times 10^6$ is the total number of $\psi(3686)$ events [14],

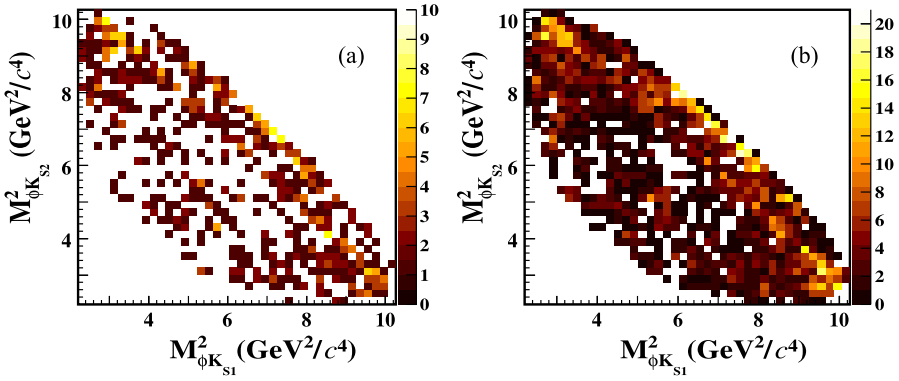

FIG. 3. Dalitz plots of $M^2_{\phi K^0_{S1}}$ vs. $M^2_{\phi K^0_{S2}}$ for the accepted candidates in (a) data and (b) BODY3 signal MC events.

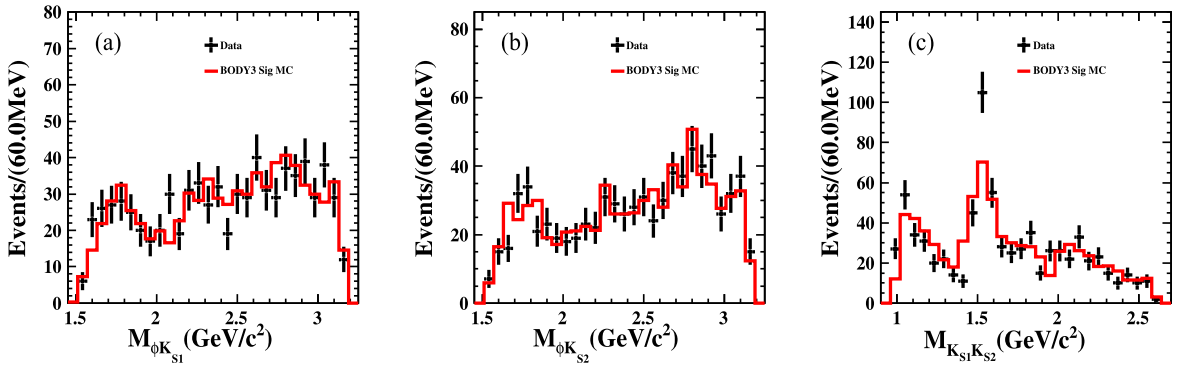

FIG. 4. Invariant mass distributions for (a) $M(\phi K^0_{S1})$ (b) $M(\phi K^0_{S2})$ (c) $M(K^0_S K^0_S)$. The points with error bars are data, the red histograms are the BODY3 signal MC.

$\mathcal{B}_{\phi\to K^+K^-}$, and $\mathcal{B}_{K^0_S\to\pi^+\pi^-}$ are the BFs of $\phi \to K^+K^-$ and $K^0_S \to \pi^+\pi^-$ quoted from the PDG [7], and $\varepsilon = (18.50 \pm 0.5)$ is the detection efficiency for $\psi(3686) \to \phi K^0_S K^0_S$. Based on these numbers, we can obtain $\mathcal{B}_{\psi(3686)\to\phi K^0_S K^0_S} = (3.53 \pm 0.20) \times 10^{-5}$.

IV. SYSTEMATIC UNCERTAINTY

The systematic uncertainties are evaluated from a variety of sources, as summarized in Table II.

The MDC tracking and PID efficiencies for kaons are studied using a control sample of $J/\psi \to K^0_S K^\pm \pi^\mp$, $K^0_S \to \pi^+\pi^-$. The difference in the tracking or PID efficiencies between data and MC simulation is assigned as individual systematic uncertainties, which is 1.0% for both tracking and PID per kaon. The PID efficiency for pions is determined based on studies of a control sample of $J/\psi \to \pi^+\pi^-\pi^0$. The difference in the PID efficiencies between the data and MC simulation, 1.4%, is assigned as the corresponding systematic uncertainty for the four pions.

The efficiency of K^0_S reconstruction is estimated using a control sample of $J/\psi \to K^*(892)^\mp K^\pm$, $K^*(892)^\mp \to K^0_S\pi^\mp$ [32]. The uncertainty includes the tracking efficiency for $\pi^+\pi^-$, the requirement of $M_{\pi^+\pi^-}$ and the requirement on

TABLE II. Relative systematic uncertainties in the BF measurement.

Source	Uncertainty (%)
$K^\pm$ tracking	2.0
$K^\pm$ PID	2.0
$\pi^\pm$ PID	1.4
K^0_S reconstruction	2.3
$N_{\psi(3686)}$	0.7
BODY3 generator	3.6
4C kinematic fit	1.3
f_c factor	0.4
MC statistics	0.5
$\mathcal{B}^{\rm PDG}(K^0_S \to \pi^+\pi^-)$	0.2
$\mathcal{B}^{\rm PDG}(\phi \to K^+K^-)$	1.0
Interference	2.1
Total	6.0

the K_S^0 decay length. The difference in the K_S^0 reconstruction efficiencies between the data and MC simulation, 1.2% per K_S^0, is taken as the systematic uncertainty, which is assigned to be 2.3%.

The number of $\psi(3686)$ events is determined from an analysis of inclusive hadronic $\psi(3686)$ decays. The uncertainty of the number of $\psi(3686)$ events, 0.7% [14], is taken as the systematic uncertainty. The systematic uncertainty of the BODY3 MC model comes from the range and the bin divisions of the input Dalitz plot. The uncertainty is estimated by changing the bin size by 20% and taking alternative ranges at the same time. The maximum change of efficiency is taken as the uncertainty, which is 3.6%.

The systematic uncertainty of the 4C kinematic fit is determined by varying the helix parameters by ± 1 standard deviation. The maximum change of signal efficiency, 1.3%, is taken as the corresponding systematic uncertainty. The systematic uncertainties due to the scale factor f_c for the continuum background originate from the uncertainty of luminosity and the uncertainty of energy dependence for the continuum cross section. The systematic uncertainty originating from the luminosity is estimated by recalculating the BF after changing the luminosity obtained by different processes. The maximum difference of the BF, 0.1%, is taken as the uncertainty. The systematic uncertainty due to the energy dependence relationship is estimated by comparing the difference between $1/s$ and $1/s^3$ [33] assumptions. The change of the remeasured BF, 0.4%, is assigned as the corresponding systematic uncertainty.

The uncertainty due to the limited MC statistics is considered as one source of systematic uncertainty. It is evaluated to be 0.5%. The uncertainties of the quoted BFs of $\mathcal{B}(K_S^0 \to \pi^+\pi^-)$ and $\mathcal{B}(\phi \to K^+K^-)$ are assigned to be 0.2% and 1.0%, respectively.

The uncertainty from the interference between $\psi(3686)$ decay and continuum production is determined by varying the measured phase angle φ by ± 1 standard deviation. The maximum change of the BF, 2.1% is taken as the corresponding systematic uncertainty.

Assuming that all sources are independent, the total systematic uncertainty is determined to be 6.0% as listed in Table II.

V. SUMMARY

Using $(448.1 \pm 2.9) \times 10^6$ $\psi(3686)$ events accumulated by the BESIII detector, the decay $\psi(3686) \to \phi K_S^0 K_S^0$ is observed for the first time. Taking the interference between $\psi(3686)$ decay and continuum production into account, its BF is measured to be $(3.53 \pm 0.20 \pm 0.21) \times 10^{-5}$, where the first uncertainty is statistical, the second one is systematic. Using the world average of $\mathcal{B}(J/\psi \to \phi K_S^0 K_S^0) = (5.9 \pm 1.5) \times 10^{-4}$ [7], the ratio between the two BFs is determined to be $\mathcal{Q}_{\phi K_S^0 K_S^0} = (6.0 \pm 1.6)\%$, which is suppressed relative to the 12% rule.

The 2.7×10^9 $\psi(3686)$ events recently collected by BESIII [8] offer an opportunity to improve the precision of $\mathcal{Q}_h$ and will lead to a better understanding of the phenomenon.

ACKNOWLEDGMENTS

The BESIII Collaboration thanks the staff of BEPCII and the IHEP computing center for their strong support. This work is supported in part by National Key R&D Program of China under Contracts No. 2020YFA0406400 and No. 2020YFA0406300; National Natural Science Foundation of China (NSFC) under Contracts No. 11635010, No. 11735014, No. 11835012, No. 11935015, No. 11935016, No. 11935018, No. 11961141012, No. 12022510, No. 12025502, No. 12035009, No. 12035013, No. 12061131003, No. 12192260, No. 12192261, No. 12192262, No. 12192263, No. 12192264, and No. 12192265; the Chinese Academy of Sciences (CAS) Large-Scale Scientific Facility Program; the CAS Center for Excellence in Particle Physics (CCEPP); Joint Large-Scale Scientific Facility Funds of the NSFC and CAS under Contract No. U1832207; CAS Key Research Program of Frontier Sciences under Contracts No. QYZDJ-SSW-SLH003 and No. QYZDJ-SSW-SLH040; 100 Talents Program of CAS; The Institute of Nuclear and Particle Physics (INPAC) and Shanghai Key Laboratory for Particle Physics and Cosmology; ERC under Contract No. 758462; European Union's Horizon 2020 research and innovation programme under Marie Sklodowska-Curie grant agreement under Contract No. 894790; German Research Foundation DFG under Contracts No. 443159800 and No. 455635585, Collaborative Research Center CRC 1044, FOR5327, GRK 2149; Istituto Nazionale di Fisica Nucleare, Italy; Ministry of Development of Turkey under Contract No. DPT2006K-120470; National Research Foundation of Korea under Contract No. NRF-2022R1A2C1092335; National Science and Technology fund; National Science Research and Innovation Fund (NSRF) via the Program Management Unit for Human Resources and Institutional Development, Research and Innovation under Contract

No. B16F640076; Polish National Science Centre under Contract No. 2019/35/O/ST2/02907; Suranaree University of Technology (SUT), Thailand Science Research and Innovation (TSRI), and National Science Research and Innovation Fund (NSRF) under Contract No. 160355; The Royal Society, UK under Contract No. DH160214; The Swedish Research Council; U.S. Department of Energy under Contract No. DE-FG02-05ER41374.

APPENDIX: FIT TO THE CROSS SECTIONS FOR $e^+e^- \to \phi K_S^0 K_S^0$ IN THE VICINITY OF $\psi(3686)$

In this appendix we describe some of the details of our fits to the cross sections for $e^+e^- \to \phi K_S^0 K_S^0$ in the vicinity of the $\psi(3686)$.

The dressed cross sections of $e^+e^- \to \phi K_S^0 K_S^0$ in the vicinity of the $\psi(3686)$ are shown in Fig. 5. A least-χ^2 fit is performed to the dressed cross section $\sigma^{\rm dressed}(s)$ using the following formula [31,34]:

$$\sigma^{\rm dressed}(s) = |A_{\rm cont}(s) + A_{\rm res}(s) \times e^{i\varphi}|^2, \qquad \text{(A1)}$$

where $\sqrt{s}$ is the c.m. energy, $A_{\rm cont}(s)$ and $A_{\rm res}(s)$ represent the amplitudes of the continuum process and $\psi(3686)$, respectively, while φ denotes the relative phase between the two amplitudes. $A_{\rm cont}(s)$ is defined as $\sqrt{C/\sqrt{s}^n}$, and the values for C and n can be determined by fitting to the $\psi(3686)$-scan data. These values of C and n will remain fixed in the fits to $\sigma^{\rm dressed}$. $A_{\rm res}(s)$ is parametrized by the single Breit-Wigner amplitude form [35].

The fitting results are shown in Fig. 5. The fit yields two solution, corresponding to a constructive interference of $(83 \pm 11)°$ and a destructive interference of $-(85 \pm 9)°$. The destructive solution is excluded from the analysis due to its significant violation of isospin symmetry with the $\psi(3686) \to \phi K^+K^-$ [7] decay.

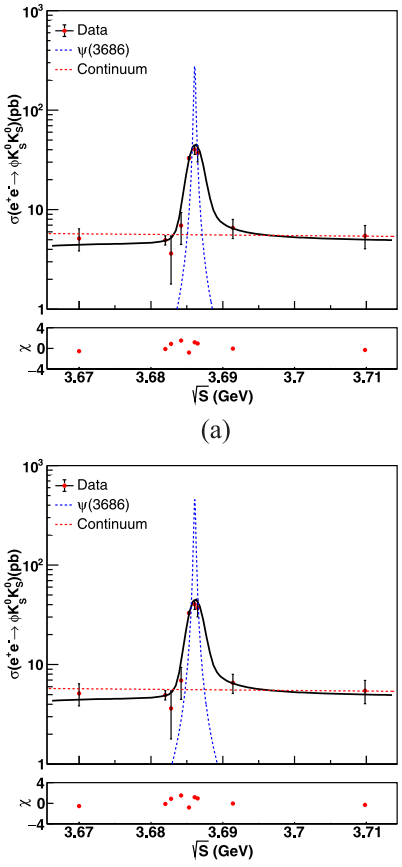

FIG. 5. The dressed cross sections of $e^+e^- \to \phi K_S^0 K_S^0$ as a function of c.m. energy for (a) constructive solution with $\phi = (83 \pm 11)°$ and (b) destructive solution with $\phi = (-85 \pm 9)°$. The two fits have the same goodness of $\chi^2/{\rm ndf} = 9.88/6$. The points with error bars are data, and the red and blue dashed curves represent the continuum contribution (with $C = (4.03 \pm 0.76) \times 10^3$ GeV$^n \cdot$ pb, $n = 5.01 \pm 0.10$) and $\psi(3686)$ contribution, respectively. The χ distributions of the two fits are shown in the bottom panel.

[1] M. Ablikim *et al.* (BESIII Collaboration), Phys. Rev. D **99**, 032006 (2019).
[2] N. Brambilla *et al.* (Quarkonium Working Group), *Heavy Quarkonium Physics* (CERN, Geneva, 2005).
[3] G. S. Abrams *et al.*, Phys. Rev. Lett. **33**, 1453 (1974).
[4] N. Brambilla *et al.*, Eur. Phys. J. C **71**, 1534 (2011).
[5] T. Appelquist and H. D. Politzer, Phys. Rev. Lett. **34**, 43 (1975).
[6] W. S. Hou and A. Soni, Phys. Rev. Lett. **50**, 569 (1983).
[7] R. L. Workman *et al.* (Particle Data Group), Prog. Theor. Exp. Phys. **2022**, 083C01 (2022).
[8] M. Ablikim *et al.* (BESIII Collaboration), Chin. Phys. C **44**, 040001 (2020).
[9] M. E. B. Franklin *et al.*, Phys. Rev. Lett. **51**, 963 (1983).
[10] J. Z. Bai *et al.* (BES Collaboration), Phys. Rev. D **69**, 072001 (2004).
[11] J. Z. Bai *et al.* (BES Collaboration), Phys. Rev. D **67**, 032004 (2003).
[12] T. K. Pedlar *et al.* (CLEO Collaboration), Phys. Rev. D **72**, 051108 (2005).
[13] R. A. Briere *et al.* (CLEO Collaboration), Phys. Rev. Lett. **95**, 062001 (2005).
[14] M. Ablikim *et al.* (BESIII Collaboration), Chin. Phys. C **42**, 023001 (2018).
[15] M. Ablikim *et al.* (BESIII Collaboration), Nucl. Instrum. Methods Phys. Res., Sect. A **614**, 345 (2010).

[16] C. H. Yu *et al.*, in *Proceedings of IPAC2016, Busan, Korea* (2016), 10.18429/JACoW-IPAC2016-TUYA01.
[17] S. Agostinelli *et al.*, Nucl. Instrum. Methods Phys. Res., Sect. A **506**, 250 (2003).
[18] Y. T. Liang *et al.*, Nucl. Instrum. Methods Phys. Res., Sect. A **603**, 325 (2009).
[19] K. X. Huang *et al.*, Nucl. Sci. Tech. **33**, 142 (2022).
[20] S. Jadach, B. F. L. Ward, and Z. Was, Phys. Rev. D **63**, 113009 (2001).
[21] D. J. Lange, Nucl. Instrum. Methods Phys. Res., Sect. A **462**, 152 (2001).
[22] R. G. Ping, Chin. Phys. C **32**, 599 (2008).
[23] J. C. Chen, G. S. Huang, X. R. Qi, D. H. Zhang, and Y. S. Zhu, Phys. Rev. D **62**, 034003 (2000).
[24] R. L. Yang, R. G. Ping, and H. Chen, Chin. Phys. Lett. **31**, 061301 (2014).
[25] E. Richter-Was, Phys. Lett. B **303**, 163 (1993).
[26] M. Ablikim *et al.* (BESIII Collaboration), Phys. Rev. Lett. **124**, 241803 (2020).
[27] M. Ablikim *et al.* (BESIII Collaboration), Chin. Phys. C **37**, 123001 (2013).
[28] M. Xu *et al.*, Chin. Phys. C **33**, 428 (2009).
[29] M. Ablikim *et al.* (BESIII Collaboration), Phys. Rev. D **87**, 012002 (2013).
[30] X. Zhou, S. Du, G. Li, and C. Shen, Comput. Phys. Commun. **258**, 107540 (2021).
[31] M. Ablikim *et al.* (BESIII Collaboration), Phys. Lett. B **791**, 375 (2019).
[32] M. Ablikim *et al.* (BESIII Collaboration), Phys. Rev. D **92**, 112008 (2015).
[33] M. Ablikim *et al.* (BESIII Collaboration), Phys. Rev. D **108**, 032004 (2023).
[34] M. Ablikim *et al.* (BESIII Collaboration), Phys. Lett. B **791**, 375 (2019).
[35] Y. P. Guo and C. Z. Yuan, Phys. Rev. D **105**, 114001 (2022).